Environmental Science & Technology

Article

pubs.acs.org/est

Importance of a Nanoscience Approach in the Understanding of Major Aqueous Contamination Scenarios: Case Study from a Recent Coal Ash Spill

Yi Yang,*[,†,§,∥] Benjamin P. Colman,[‡,∥] Emily S. Bernhardt,[‡,∥] and Michael F. Hochella*[,†]

[†]The Center for NanoBioEarth, Department of Geosciences, Virginia Tech, Blacksburg, Virginia 24061, United States

[‡]Biology Department, Duke University, Durham, North Carolina 27708, United States

[§]Department of Geosciences, East China Normal University, 3663 North Zhongshan Road, Shanghai, 200062, China

[∥]Center for the Environmental Implications of NanoTechnology (CEINT), Duke University, Durham, North Carolina 27517, United States

Supporting Information

ABSTRACT: A coal ash spill that occurred from an ash impoundment pond into the Dan River, North Carolina, provided a unique opportunity to study the significance and role of naturally occurring and incidental nanomaterials associated with contaminant distribution from a large-scale, acute aquatic contamination event. Besides traditional measurements of bulk watercolumn and sediment metal concentrations, the nanoparticle (NP) analyses are based on cross-flow ultrafiltration (CFUF) and advanced transmission electron microscopy (TEM) techniques. A drain pipe fed by coal ash impoundment seepage showed a high level of arsenic, with concentrations many times over the EPA limit. The majority of the arsenic was found sorbed to large aggregates dominated by incidental iron oxyhydroxide (ferrihydrite) NPs, while the remainder of the arsenic was truly dissolved. These ferrihydrites were probably formed in situ where Fe(II) was leached through subsurface flowpaths into an aerobic environment, and further act as a significant contributor to the elevated As concentrations in downstream sediments after the spill. In addition, we discovered and describe a photocatalytic nano-TiO_2 phase (anatase) present in the coal ash impacted river water that was also carrying/transporting transition metals (Cu, Fe), which may also have environmental consequences.

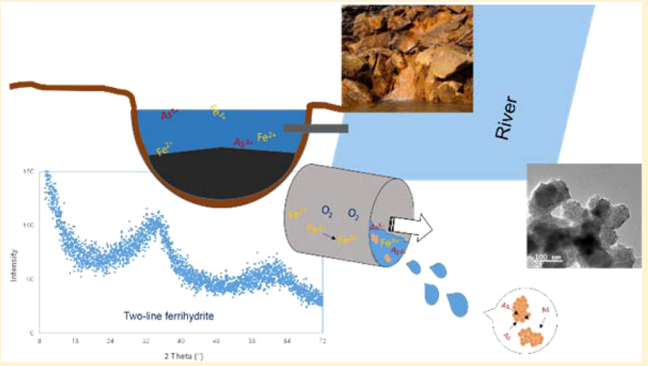

INTRODUCTION

It is becoming increasing apparent that naturally occurring and anthropogenic incidental nanomaterials play an important and often completely overlooked role in regulating the behavior of contaminants in complex aquatic systems. This statement is applicable to both manmade aquatic systems, such as nanomaterials in water treatment plants and distribution systems,[1−3] and natural aquatic systems, such as rivers and groundwater.[4−7] What has been generally missing is an example of a major, acute aqueous contaminant spill where the central role of naturally occurring and incidental nanomaterials has been clearly delineated. Our opportunity to study this underrepresented type of impact in a major aqueous contamination scenario came in February 2014 during a coal ash spill into the Dan River near the town of Eden, North Carolina. Although this spill was considerably smaller than previously studied coal ash spills in the North Carolina/Tennessee areas,[8,9] it was still a major event. The resulting flow of ash and water was estimated to contain 27 million gallons of water and 30 000−39 000 tons of coal ash flowing into the Dan River from February 2 to 8, 2014, when the leak was finally and successfully capped.[10]

Coal combustion residues (CCRs) can cause elevated concentrations of toxic metals in surface water (streams, rivers, and lakes), and potentially in groundwater.[11,12] Previous studies of coal ash spills have documented long-term chemical impacts that may result in long-term environmental and health impacts on these aquatic systems.[9,12] There has been limited research on these long-term impacts, however a recent study concluded that the amount of toxic metal released from coal ash and its further mobility in an aquatic system are considered the key factors that control the environmental risk.[8]

Whereas regulations in the United States for many contaminants commonly found in ash spills are based on total concentrations, studies on water quality and pollutants following coal ash spills often differentiate between solid

Received: November 19, 2014
Revised: February 10, 2015
Accepted: February 17, 2015
Published: February 17, 2015

DOI: 10.1021/es505662q
Environ. Sci. Technol. 2015, 49, 3375−3382

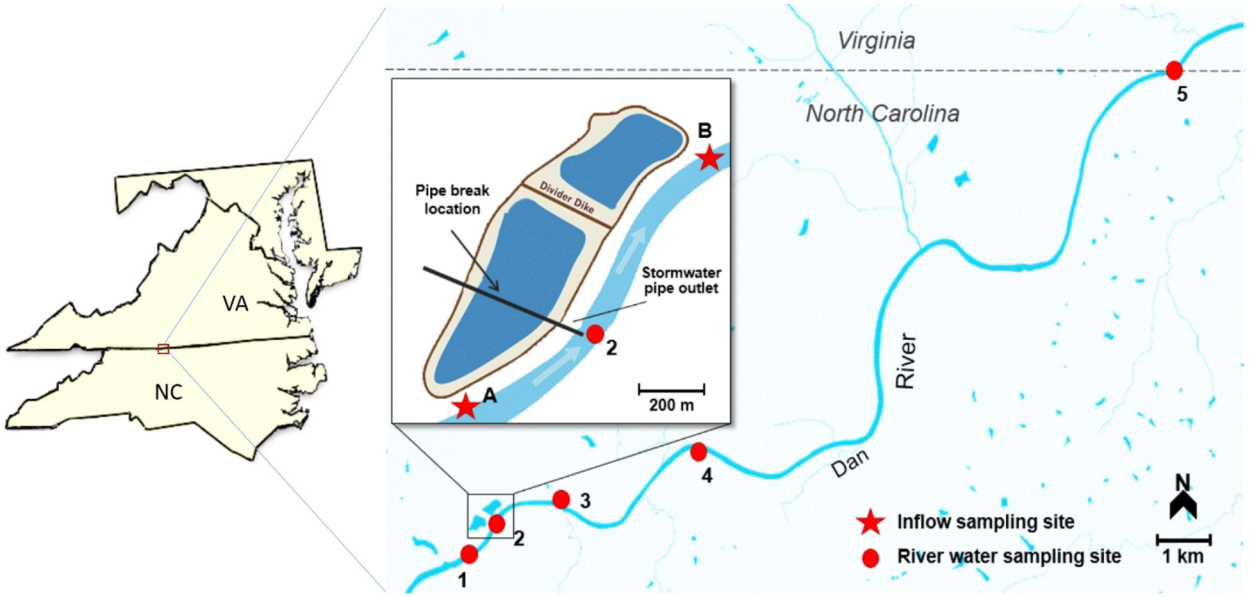

Figure 1. Map of the sampling sites along the Dan River (modified according to the Dan River steam station diagram, Duke Energy[17]).

particulate matter (SPM) and dissolved materials by separating them using membrane filters (e.g., having a pore size of 0.45 μm). In fact, the "dissolved" phase present in the filtrate of natural waters is a complex mixture including a range of sizes of colloids, nanoparticles (NPs), and the truly dissolved phase.[13,14] In the last several years, growing attention has been given to NPs due to their inherent reactivity with contaminants and their implications for contaminant mobility.[15,16] These NPs can be transported for long distances and serve as carriers for contaminants that may significantly alter their fate and transport relative to standard geochemical assumptions, calculations, and models.

To systematically assess the role of NPs associated with toxic metals in a major aqueous contamination scenario, water samples from the Dan River and two inflows to the Dan River from the coal ash impoundment areas were sequentially separated using cross-flow ultrafiltration (CFUF) into >0.45 μm, <0.45 μm, 1 kDa−0.45 μm, and <1 kDa fractions, where 1 kDa is roughly equivalent to 1 nm in size. Major and trace element concentrations were analyzed in each fraction. To achieve our goal, it was necessary (1) to determine the distribution of metals in different fractions of water; (2) to find and identify the dominant NPs in inflows from the impoundment area, the river water, and river sediment samples; and (3) to closely examine the association of toxic metals with NPs. To characterize colloids and NPs, we used a variety of X-ray and electron based techniques including X-ray diffraction (XRD), transmission electron microscopy (TEM), scanning TEM (STEM), and selected area electron diffraction (SAED) analysis.

MATERIALS AND METHODS

Sample Collection. On February 9, 2014, the day after the spill was capped, water and sediments were sampled from the Dan River in the vicinity of the Dan River Steam Station. Water was sampled from the river channel above the dam at the power plant (0.6 km upstream of the spill site, Site 1; Figure 1), at the spill site within the perimeter of a floating sediment curtain that was deployed in the water surrounding the area of the river around the pipe that had been leaking (Site 2), and at 1.1, 3.6, and 14 km downstream (Sites 3, 4, and 5, respectively). Water was sampled by using an acid-washed high-density polyethylene bucket to collect surface water subsamples that were combined to fill a 20-L polycarbonate carboy. Water was also collected from two preexisting inflows to the Dan River associated with the Dan River Steam Station. The first was a discharge just upstream of the primary ash basin (0.5 km upstream; Inflow A in Figure 1) fed by a mixture of seep water and stormwater. The second inflow was a stream that runs along the earthen dam of the secondary ash basin and into the Dan River (0.5 km downstream of the spill; Inflow B). Detailed information on the sampling sites and two inflows has been provided in the Supporting Information (SI).

Five sediment samples were collected along the river at a subset of the water sampling locations using a plastic scoop, with the goal of collecting the top 5−10 cm of sediment. Two sampling sites were located immediately below the spill site, with samples being collected both within the spill mediation curtain and outside of the curtain. Sediments were collected from three additional sites that were 0.5, 1.1, and 2 km downstream of the spill site.

Filtration of Water Samples. Bulk water samples were filtered using a cross-flow ultrafiltration (CFUF) system (Pellicon System, Millipore, USA) equipped with membranes of different pore sizes. Water samples were sequentially separated through a Millipore 0.45-μm Pellicon 2 HVMP membrane and a 1-kDa regenerated cellulose Pellicon 2 PLAC ultrafiltration membrane as described in SI Figure S1. The retentate flow containing the colloids was directed back to the feed container so that it became more concentrated with time, while the permeate flow was collected separately containing the truly dissolved phases. A concentration factor (cf) (ratio of the volume of the initial sample to the retentate volume) of 25 was chosen to optimize for a reliable determination of the colloidal pool for trace metals (see details in the SI).[13] In this way, each original water sample was separated into >0.45 μm, <0.45 μm, 1 kDa−0.45 μm, and <1 kDa fractions, in which >0.45 μm and 1 kDa−0.45 μm fractions are concentrated retentates which are referred to in this paper as SPM and colloidal suspension, respectively. The CFUF system was initially cleaned using 0.1

DOI: 10.1021/es505662q
Environ. Sci. Technol. 2015, 49, 3375−3382

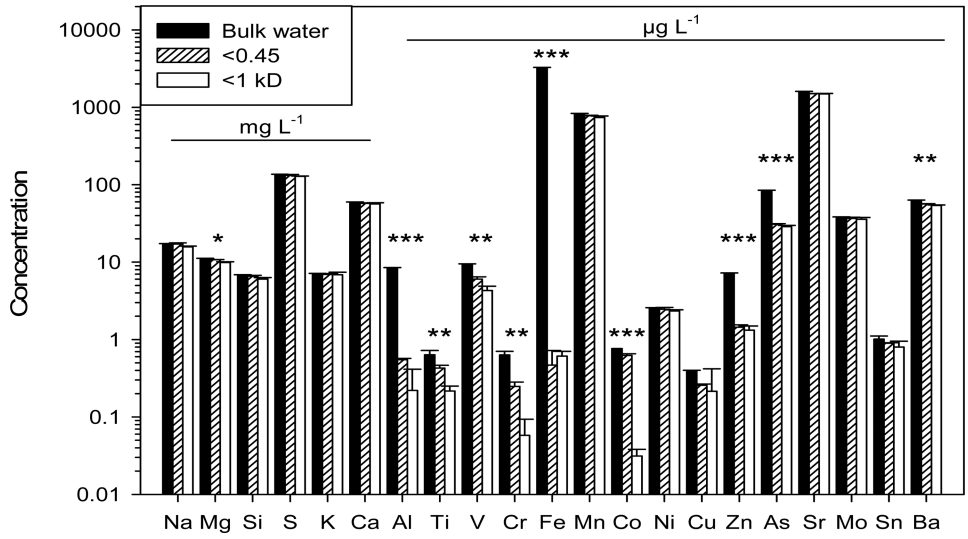

Figure 2. Concentrations of major elements (Na, Mg, Si, K, and Ca in mg/L) and trace metals (Al, Ti, V, Cr, Fe, Mn, Co, Ni, Cu, Zn, As, Sr, Mo, Sn, and Ba in μg/L) in different fractions from Inflow A. Differences within an element between size classes are denoted as being significant at $p < 0.05$ (*), $p < 0.01$ (**), and $p < 0.001$ (***).

M HNO_3 and 0.1 M NaOH solution for 30 min, respectively. Prior to loading each sample, the system was thoroughly rinsed with 10 L of Milli-Q water and 1 L of feedwater sample.

The recoveries of all the elements analyzed in water by CFUF separation were 74.1−108.6%, with the exception of Ti (for which we recovered only 23−86%). These recoveries are considered satisfactory due to the unavoidable system loss or contamination. The poor recovery of Ti was a result of the loss to the separation system and poor digestion efficiency with HNO_3 and even with 2% aqua regia, as Ti oxides are extremely refractory phases.

ICP-MS Analysis. Major and trace element standards were purchased from High-Purity Standards (Charleston, SC.). Water samples and calibration standards were prepared in a matrix of 2% nitric acid by volume in duplicates. Bulk water and >0.45-μm fractions were acid digested according to Standard Method 3030F.[18] This method is satisfactory for most metals but is inefficient for titanium oxides, which are insoluble even under strong acidic condition. Sediment samples were acid digested in duplicates following EPA Method 3050B. Major and trace element concentrations were analyzed using a Thermo Electron X-Series inductively coupled plasma mass spectrometer (ICP-MS) per Standard Method 3125-B.[18]

Electron Microscopy Analysis. Sediment and the retentate of the >0.45-μm fraction of inflow samples were investigated using an environmental scanning electron microscope (ESEM, FEI Quanta 600 FEG) equipped with an energy-dispersive X-ray spectrometer (EDS, QUANTAX 400, Bruker). Selected colloidal solution samples were placed onto a 300-mesh copper TEM grid with lacey carbon support film (Electron Microscopy Sciences, PA). Morphology, aggregation, chemistry, and crystal structure of the NPs in the colloidal solution (1 kDa−0.45 μm fraction) were investigated using a JEM 2100 TEM/STEM (JEOL Corporation) operating at 200 kV and equipped with an energy dispersive X-ray (EDX) spectrometer. Electron diffraction patterns of the crystalline and semicrystalline phases were recorded in selected area electron diffraction (SAED) mode.

XRD. The SPM suspension from Inflow A was pipetted onto a zero background sample holder and analyzed by a Rigaku MiniFlex X-ray diffractometer (Ni-filtered Cu Kα radiation, scanned between 10° and 80° 2θ at a scan rate of 0.02° 2θ s^{-1}). All raw data files were converted to an Excel file from which the relative intensity was plotted versus 2θ.

RESULTS AND DISCUSSION

The highest concentrations of contaminants in water samples associated with CCR were measured not at the site of the spill, but from the two inflows which enter the Dan River both upstream (Inflow A) and downstream (Inflow B) of the ash containment basins. Concentrations in <0.45-μm water of Na, S, Al, Cr, Mn, Co, As, Sr, and Mo were all significantly higher in both inflows than in any of the sampling locations within the Dan River (SI Table S2, t-test, $p < 0.05$). For both inflows we found that the majority of the trace metals were in the <1-kDa fractions, which are considered to be the truly dissolved metals.

Characterization of Inflows. As mentioned in the site description in the Supporting Information, Inflow A is fed by a mixture of seepage from the primary ash basin, yard drains, and stormwater. Although the flux of water may have been driven by stormwater, the sample from Inflow A had high concentrations of known coal combustion constituents in bulk water including Fe, Mn, As, Sr, Mo, and Ba. Of particular concern was arsenic in the bulk water. At 85 μg As L^{-1}, the arsenic concentration in Inflow A was more than eight times the US EPA Maximum Contaminant Level (MCL) of 10 μg L^{-1}.[19] Whereas the MCL applies to unfiltered water, it is noteworthy that filtered water concentrations were 30 μg/L in the <0.45-μm fraction and slightly lower (28.8 μg/L) in the <1-kDa fraction, both of which were still well in excess of the MCL. Although the Fe concentration was 3250 μg/L in the unfiltered water, there was no measurable iron in the <0.45-μm fraction, indicating that nearly all of the Fe was present in the SPM fraction (Figure 2). The mass balance of elements was calculated by including the SPM, colloidal, and dissolved phases. Significant proportions of the total aluminum and arsenic present in the bulk sample was also found in this largest size fraction (SI Figure S2). For all other major elements, we found no significant difference between concentrations in bulk

DOI: 10.1021/es505662q
Environ. Sci. Technol. 2015, 49, 3375−3382

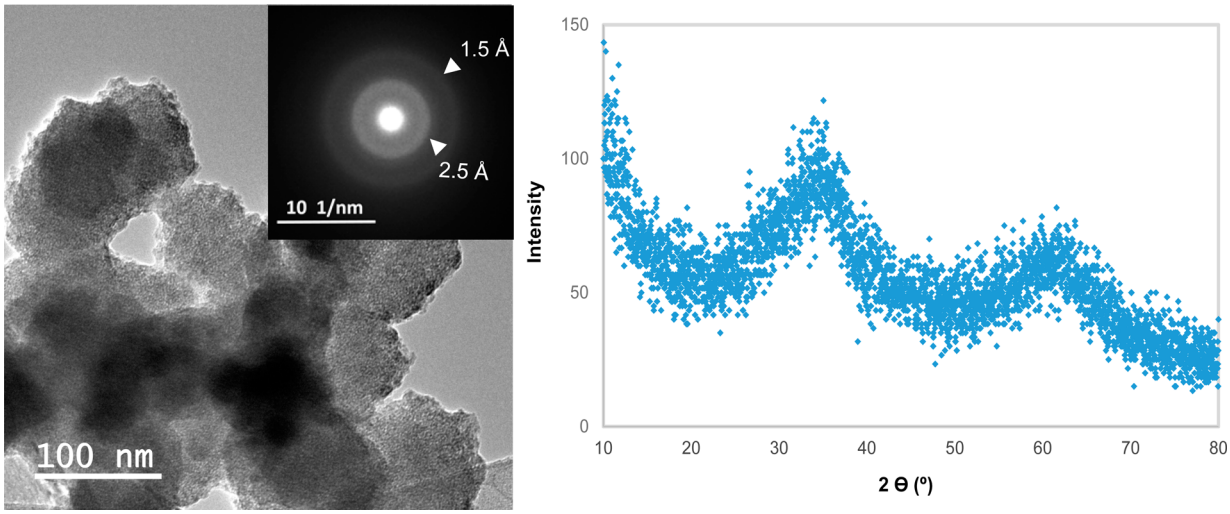

Figure 3. TEM and SAED images (left) and XRD pattern (right) of >0.45-μm fraction in the effluent from the coal ash impoundment collected at Inflow A (sampling site A in Figure 1) showing evidence for two-line ferrihydrite.

water, <0.45-μm, and <1-kDa fractions, revealing these elements were mostly in the dissolved phase.

The SPM fraction retained by a 0.45-μm filter had an average hydrodynamic diameter of 1641 nm (1.6 μm) as measured by dynamic light scattering (SI Figure S3). Further characterization of the particles that made up the SPM fraction by TEM-EDS showed that these were predominantly iron-rich particles that were intimately associated with both Si and As (SI Figure S4). The iron particles in the SPM fraction were shown by XRD to be mostly two-line ferrihydrites with diffuse peaks centered at *d*-spacings of 1.5 and 2.5 Å. This was further confirmed by TEM coupled with SAED (Figure 3). The finding that these ferrihydrite particles tended to form large aggregates is consistent with the finding that the particles had a zeta potential of 0.05 mV suggesting that they were near their point of zero charge and thus destabilized.

The presence of large aggregates of arsenic-rich ferrihydrites in water from Inflow A was likely the result of a combination of processes. In the primary coal ash basin, anaerobic conditions in the ash material can cause the reduction and solubilization of metals like iron and arsenic. Leaching of reduced metals through subsurface flowpaths into an aerobic environment such as the discharge pipe and surface water would allow for oxidation of Fe(II) to Fe(III) through biological and geochemical pathways, and precipitation of ferric minerals. In the case of iron oxidation, the first phase to precipitate in hydrolysis is usually ferrihydrite. Ferrihydrite is a poorly crystalline iron oxyhydroxide having an approximate formula of $Fe_{10}O_{14}(OH)_2$[20] and exceptionally high surface area. Its formation is favorable given the circumneutral pH and 5 °C temperature of the inflow, while its high surface area would have been conducive to sorption of As. Meanwhile, the near zero zeta-potential allows these particles to aggregate. Although there was extensive deposition of ferrihydrite on the rocks lining the inflow channel (SI Figure S5), our data show that it was also entering the stream at high concentrations. Given that 64% of the total arsenic entering the stream from this inflow was associated with ferrihydrite-dominated aggregates, the formation, transformation, and transport of ferrihydrite-associated arsenic is likely the key to understanding its fate and impacts in the stream ecosystem.

The concentrations of most constituents were in general lower in Inflow B than in Inflow A (SI Table S1), but concentrations of the toxic metalloid As in Inflow B was 11.6 μg/L in the unfiltered water, still above the EPA drinking water standard of 10 μg/L. In contrast to Inflow A where the majority of As was present in the SPM fraction, nearly all (97.5%) of the arsenic entering the stream at Inflow B was in the <1-kDa fraction (SI Figure S2). This may be driven by differences in the concentration and form of iron in the two inflows. Inflow A had an order of magnitude higher iron concentration than Inflow B in the bulk water, with no detectable iron in the <0.45-μm fractions. Inflow B had 41% of its iron in the <0.45-μm fraction, for which 21% was in the colloidal fraction; there was no evidence of ferrihydrite NPs in the SPM or colloidal fraction using SEM or TEM. This finding can also explain the higher proportion of As in the <1-kDa fraction compared to that in Inflow A.

Characterization of Metals in the Dan River Surface Water. When comparing Site 2 (spill site) with all other surface water sites, there was significantly higher Al, Fe, Zn, Mo, Ti, and Ni within the sediment curtain installed to contain the spill (SI Table S1, Tukey-HSD, $p < 0.05$). These elevated concentrations may have been due to either residual spill water or the longer residence time of water in contact with spilled ash within the curtain compared to other sampling sites in the main channel. However, these signals did not seem to propagate downstream, suggesting that the effects of the spill on water column contaminant concentrations were diluted by the Dan River below established toxicity standards within 1 day of the spill being stopped. Arsenic concentrations throughout the river surface waters were 0.7−1.2 μg/L, with a mean value of 0.86 μg/L, which is in agreement with the data reported by concurrent EPA investigations at the site.[21]

The distribution of all analytes (with the exception of Ti), based on their mass balance among SPM, colloidal, and the truly dissolved water fractions shows that most of the major components were found in the dissolved fraction (SI Figure S6). More than 97% of Na, Mg, Si, K, and Ca are in the <1-kDa fraction, as was 87−96% of S. The same was true for most of the trace metals; more than 90% of V, Mn, Sr, Mo, Sn, and Ba were in the <1-kDa fractions and 88−95% of As was in the dissolved phase. In contrast, Al, Fe, and Cu were more

DOI: 10.1021/es505662q
Environ. Sci. Technol. 2015, 49, 3375−3382

concentrated in the SPM and colloidal fractions (SI Figure S6). Across all sites, Al was dominantly found in the SPM phase, but its concentration in the SPM phase went from a low of 51% at Site 1 to a high of 98% of total Al at Site 5. Colloidal Al showed the opposite pattern of SPM and went from a maximum of 43.9% of total Al at Site 1 in the colloidal fraction down to 0.6% at Site 5. There was less of a clear spatial trend for Cu or Fe, which both had strong colloidal components ranging from 23 to 68% for Cu, and 16 to 46% for Fe. The high concentration of Al, Fe, and Cu in the colloidal size range suggests either Al-, Fe-, and Cu-rich NPs or high affinities of these trace metals to NPs in these fractions.

NPs Identified in the Colloidal Fractions of Water Samples. Recoveries of Ti ranged from 23 to 86% following CFUF separation owing to loss to the separation system and poor digestion even with 2% aqua regia. Even so, Ti concentrations were much greater than the detection limit of 0.3 μg/L in all fractions >1 kDa, and they were all under the detection limit in the <1-kDa fractions showing that Ti was limited to the SPM and colloidal fractions. In the SPM fraction, Ti concentrations were 8.0−21.1 μg/L and 1.9−9.4 μg/L in the 1-kDa−0.45-μm fractions. Given Ti-bearing phases' exceptionally low solubility and presence in the colloidal fraction, we predicted that much of this Ti would be present as TiO_2-NPs.

This prediction was confirmed when subsequent TEM identified titanium dioxide particles in the colloidal fraction of river water samples. TiO_2-NPs were in aggregates with individual primary particles in the size range of 20−250 nm. The crystal structure was consistent with anatase TiO_2, as identified by SAED which showed *d*-spacings of 3.53, 2.43, and 2.33 matching anatase *d*-spacings for (1 0 1), (1 0 3), and (1 1 2).[22] In addition, Cu, Al, and Fe were found to be associated with TiO_2 (SI Figure S7). Although copper grids were used for mounting the TEM samples, there were much higher X-ray counts generated by the TiO_2 particle-associated Cu compared to that of the background. (In addition, the Cu signal from TiO_2 was confirmed by mounting one of the samples on a gold grid; the Cu X-ray signal from TiO_2 is still present.) In an earlier study, Kim et al.[23] showed that rutile NP aggregates in sewage sludge had an affinity with spiked Ag. Titanium oxides have also been suggested to be associated with other metals such as Pb and Zn in sediments according to correlation analyses.[24] By column breakthrough tests, TiO_2 was observed as a carrier and facilitated the transportation of Cu.[25] In the present study we show in environmental samples that TiO_2−NPs (anatase) sorb other metals such as Cu, Fe, and Al, thus acting as a carrier which can alter the transport, fate, and bioavailability of these metals.

Iron oxides were also identified by TEM-EDS in the 1-kDa−0.45-μm fractions of the river water samples downstream of the spill site (SI Figure S8). In general, these particles had either a spherical or rod-like shape, with particle sizes in the range of 30−100 nm. Notably absent were both ferrihydrite- and iron oxide-associated arsenic. Instead, the rod-like iron oxides were shown by SAED to have *d*-spacings of 4.18 and 2.7 Å, which matches those for the (1 1 0) and (1 3 0) planes of goethite,[26] while spherical particles had *d*-spacings of 3.69, 2.71, 2.53, and 2.23 Å, which are in agreement with those for the (0 1 2), (1 0 4), (1 1 0), and (1 1 3) planes of hematite.[27] These iron oxides could be naturally occurring, or related to the ultrafine particles released by coal ash as both goethite and hematite were also observed in coal ash samples.[28]

Elevated Arsenic in Sediments. Coal ash from the spill was, as anticipated, found to be mixed with downstream river sediments as evidenced by their gray and black color (SI Figure S9). This is also supported by the sediment trace metal chemistry, which was comparable to values reported by the EPA for coal ash in the primary impoundment and sediment at the spill site including elevated Fe, Mn, and Ba.[29,30] Elevated arsenic concentrations were also found in the downstream river sediments in the range of 14.8−29.2 μg/g (SI Table S3), which overlaps the range for coal ash in the primary impoundment (17−60.8 μg As g^{-1}). Not surprisingly, this is dramatically higher than arsenic concentrations in upstream sediment control samples (0.2 μg As g^{-1}) reported by the EPA.[30] Although there is no regulatory guideline for arsenic in sediments in the United States, the Canadian Council of Ministers of the Environment (CCME) has provided an interim sediment quality guideline (ISQG) of 5.9 μg/g and probable effect level (PEL) of 17 μg/g for arsenic.[31] The arsenic concentrations in the sediments one week after the coal ash spill were all higher than the ISQG and generally higher than this PEL, which indicates an elevated risk of adverse effects on sediment-dwelling organisms and the fish and wildlife that may feed on them.[31]

Coal ash is a well-known source of arsenic, with concentrations in coal fly ash worldwide in the range of 2.3−1700 μg/g.[32] Extremely high concentrations of arsenic (up to 35 000 μg/g) have been reported in some unburnt coal.[33] The coal ash from the field site described in this paper had an As concentration of up to 60.8 μg/g according to a report by the US EPA.[29] The As trapped in coal plant scrubbers serves as a significant contribution of As to coal slurry impoundments and from there to impoundment outflows or leaks (e.g., Inflow A) and, through catastrophic spills, to river sediments. Just as we found in Inflow A, arsenic associated with ferrihydrite aggregates were found in all of the downstream river sediments by SEM and TEM (SI Figure S10). However, there was no overall correlation between arsenic and iron concentrations (r = 0.4, p = 0.5) in the coal ash-influenced sediments. Regardless of whether these ferrihydrite particles were associated with the coal ash or only from Inflow A, it suggests that ferrihydrite may be an important source and carrier of arsenic in the sediment. In addition, studies on coal ash show that As (V) is found predominantly as arsenate,[34] which is known to be adsorbed onto iron oxides and silicates in coal ash.[34−36] Therefore, arsenic-containing ferrihydrite aggregates and particles would be expected to have different bioavailability and transport behaviors relative to arsenic in coal ash. It is known that ferrihydrite can sequestrate As in solution both through an inner sphere surface complex and an outer sphere surface complex,[37] and it can release As by reductive dissolution irrespective of whether As is coprecipitated on or absorbed below its surface.[38,39] Moreover, as ferrihydrite-associated As is deposited in river sediments, anoxic conditions should favor the reduction of adsorbed arsenate to arsenite,[40] which is more toxic to organisms.[41]

Environmental Implications. In addition to detailing the short-term aftermath of the Dan River Steam Station coal ash spill, we also described highly elevated concentrations of a number of trace metals, including arsenic, in inflows to the Dan River from the coal ash basins. Such high concentrations provide chronic sources of toxic and potentially toxic metals to aquatic ecosystems downstream. About 64% of the arsenic in the upstream river inflow from the impoundment areas (Inflow

DOI: 10.1021/es505662q
Environ. Sci. Technol. 2015, 49, 3375−3382

A) was mostly associated with ferrihydrite which was probably formed in situ where Fe(II) was leached through subsurface flowpaths into an aerobic environment. These iron oxyhydroxide NPs aggregate into the SPM fraction and act as carriers of arsenic between the ash basins and the river. In the river, the aggregates increase the rate of settling and accumulation in river sediments compared to what would be expected for dissolved As. This is important to know because arsenic that ends up in the sediments is, of course, not permanently removed from the ecosystem. There are several mechanisms by which this ferrihydrite-associated arsenic can be released into dissolved and more toxic forms. Bound arsenate may be released as the more toxic dissolved arsenite under hypoxic or anoxic conditions. Arsenic can be competitively displaced on ferrihydrite binding sites by organic or inorganic compounds with a higher binding affinity.[42−44] Arsenic may also be released or transformed by microbial activity and also by changes in water conditions,[45−47] such as pH, temperature, redox potential, or the occurrence of other compounds that can catalyze the transformation of the metastable ferrihydrite.

In addition to the aggregates of ferrihydrite NPs in Inflow A and the river sediment, titanium oxides in the form of anatase were identified in the colloidal fractions of all river samples. These anatase NPs could be from wastewater discharge or stormwater generated by the town of Eden, NC several km further upstream, or from coal combustion processes. Prior studies have suggested that TiO_2-NPs leached from exterior paint and TiO_2-NP in sunscreens could be important inputs of TiO_2 into aquatic systems.[2,48] It is notable that the anatase polymorph of TiO_2 was identified in the present study, although only rutile TiO_2-NPs have been recently found in sewage sludge.[23] Anatase is mostly used as a catalyst due to its very high photoreactivity, and it is considered potentially more toxic than rutile. It has been reported that anatase can generate more than six times more reactive oxygen species (ROS) than rutile after UV irradiation[49] and can induce DNA damage and alterations.[50,51] Recent cytotoxicity studies show that anatase NPs also exhibit significant acute toxicity to aquatic bacteria compared to rutile.[52,53] The occurrence of anatase NPs in the Dan River may thus have direct environmental impacts. Perhaps more importantly, we found that several trace metals (Al, Fe, and Cu) were associated with these titanium oxide NPs, likely affecting their transport and fate and with potentially important, but as yet unstudied, consequences for their bioavilability and toxicity. Laboratory tests have shown that copper sorbed to nano-TiO_2 has greatly enhanced toxicity to *Daphnia magna* due to a significant increase in copper bioaccumulation in this organism.[54] Whether such mechanisms apply for other metals and in the more complex physicochemical environment of natural systems is an important question for further study.

By applying nanoscience perspectives and tools to the study of this unfortunately common type of significant contaminant spill we have been able to show that NPs are an important component of the contaminant mixture within a coal ash spill. Because the transport, bioavailability, toxicity, and ecological impact of a toxin depends not only on its concentration but also on its form, this work points out the importance of examining the role of nanoscale contaminants as an important component of both existing and future aquatic ecosystem pollution scenarios.

■ ASSOCIATED CONTENT

Supporting Information

More detailed information on the sampling sites and the sample collection procedures, along with supplementary graphs and figures. This material is available free of charge via the Internet at http://pubs.acs.org.

■ AUTHOR INFORMATION

Corresponding Authors

*E-mail: yyang@geo.ecnu.edu.cn.
*E-mail: hochella@vt.edu.

Notes

The authors declare no competing financial interest.

■ ACKNOWLEDGMENTS

This paper was improved by the comments from the anonymous reviewers and the associated editor who handled this publication. We truly appreciate their efforts. A grant from the National Science Foundation (NSF) and the Environmental Protection Agency (EPA) in the United States under NSF Cooperative Agreement EF-0830093, entitled Center for the Environmental Implications of Nanotechnology (CEINT), provided major financial support for this study. Additional support was provided by the National Natural Science Foundation of China (41271473 and 41130525) and the Fundamental Research Funds for the Central Universities, the Open Foundation of East China Normal University. We thank Dr. Jeffrey L. Parks for the ICP-MS analysis and Stephen McCartney and Christopher Winkler in the Nanoscale Characterization and Fabrication Laboratory at Virginia Tech. We also thank the Yadkin Valley Riverkeepers, and the Waterkeeper Alliance for helping us access these sites, and Jessica Brandt and Anna Fedders for their assistance in sampling.

■ REFERENCES

(1) Kim, B.; Park, C.; Murayama, M.; Hochella, M. F. J. Discovery and characterization of silver sulfide nanoparticles in final sewage sludge products. *Environ. Sci. Technol.* **2010**, *44*, 7509−7514.
(2) Kaegi, R.; Ulrich, A.; Sinnet, B.; Vonbank, R.; Wichser, A.; Zuleeg, S.; Simmler, H.; Brunner, S.; Vonmont, H.; Burkhardt, M.; Boller, M. Synthetic TiO_2 nanoparticle emission from exterior facades into the aquatic environment. *Environ. Pollut.* **2008**, *156* (2), 233−9.
(3) Ma, R.; Levard, C.; Judy, J. D.; Unrine, J. M.; Durenkamp, M.; Martin, B.; Jefferson, B.; Lowry, G. V. Fate of zinc oxide and silver nanoparticles in a pilot wastewater treatment plant and in processed biosolids. *Environ. Sci. Technol.* **2014**, *48* (1), 104−112.
(4) Bertsch, P. M.; Seaman, J. C. Characterization of complex mineral assemblages: Implications for contaminant transport and environmental remediation. *Proc. Natl. Acad. Sci. U.S.A.* **1999**, *96*, 3350−3357.
(5) Johnson, C. A.; Freyer, G.; Fabisch, M.; Caraballo, M. A.; Ksel, K.; Hochella, M. F. Observations and assessment of iron oxide and green rust nanoparticles in metal-polluted mine drainage within a steep redox gradient. *Environ. Chem.* **2014**, *11* (4), 377.
(6) French, R. A.; Caraballo, M. A.; Kim, B.; Rimstidt, J. D.; Murayama, M.; Hochella, M. F. The enigmatic iron oxyhydroxysulfate nanomineral schwertmannite: Morphology, structure, and composition. *Am. Mineral.* **2012**, *97* (8−9), 1469−1482.
(7) Novikov, A. P.; Kalmykov, S. N.; Utsunomiya, S.; Ewing, R. C.; Horreard, F.; Merkulov, A.; Clark, S. B.; Tkachev, V. V.; Myasoedov, B. F. Colloid transport of plutonium in the far-field of the Mayak Production Association, Russia. *Science* **2006**, *314* (5799), 638−41.
(8) Ruhl, L.; Vengosh, A.; Dwyer, G. S.; Hsu-Kim, H.; Deonarine, A. Environmental impacts of the coal ash spill in Kingston Tennessee: An 18-month survey. *Environ. Sci. Technol.* **2010**, *44*, 9272−9278.

DOI: 10.1021/es505662q
Environ. Sci. Technol. 2015, 49, 3375−3382

(9) Ruhl, L.; Vengosh, A.; Dwyer, G. S.; Hsu-Kim, H.; Deonarine, A.; Bergin, M.; Kravchenko, J. Survey of the potential environmental and health impacts in the immediate aftermath of the coal ash spill in Kingston, Tennessee. *Environ. Sci. Technol.* **2009**, *43* (16), 6326−6333.
(10) U.S. Environmental Protection Agency. Region 4 and Region 3. www.duke-energy.com/pdfs/Duke_EPA_Agreement.pdf (accessed 2014).
(11) Rowe, C. L.; Hopkins, W. A.; Congdon, J. D. Ecotoxicological implications of aquatic disposal of coal combustion residues in the United States: A review. *Environ. Monit. Assess.* **2002**, *80*, 207−276.
(12) Ruhl, L.; Vengosh, A.; Dwyer, G. S.; Hsu-Kim, H.; Schwartz, G.; Romanski, A.; Smith, S. D. The impact of coal combustion residue effluent on water resources: A North Carolina example. *Environ. Sci. Technol.* **2012**, *46* (21), 12226−12233.
(13) Wilkinson, K. J.; Lead, J. R. *Environmental Colloids and Particles: Behaviour, Separation and Characterisation*; John Wiley and Sons: Chichester, U.K., 2007.
(14) Hochella, M. F., Jr.; Lower, S. K.; Maurice, P. A.; Penn, R. L.; Sahai, N.; Sparks, D. L.; Twining, B. S. Nanominerals, mineral nanoparticles, and earth systems. *Science* **2008**, *319*, 1631−1635.
(15) Yang, Y.; Fu, J.; Peng, H.; Hou, L.; Liu, M.; Zhou, J. L. Occurrence and phase distribution of selected pharmaceuticals in the Yangtze Estuary and its coastal zone. *J. Hazard. Mater.* **2011**, *190* (1−3), 588−96.
(16) Wigginton, N. S.; Haus, K.; Hochella, M. F., Jr. Aquatic environmental nanoparticles. *J. Environ. Monit.* **2007**, *9*, 1306−1316.
(17) June Coal Ash News. http://www.coalashchronicles.com/tag/dan-river (accessed 2014).
(18) Clesceri, L. S.; Greenberg, A. E.; Eaton, A. D. *Standard Methods for the Examination of Water and Wastewater*, 20th Ed.; American Public Health Association: Washington, DC.
(19) U.S. Environmental Protection Agency. *National Primary Drinking Water Regulations: Maximum Contaminant Levels*; http://www.epa.gov/safewater/contaminants/index.html; no. 1 (accessed 2014).
(20) Michel, F. M.; Ehm, L.; Antao, S. M.; Lee, P. L.; Chupas, P. J.; Liu, G.; Strongin, D. R.; Schoonen, M. A.; Phillips, B. L.; Parise, J. B. The structure of ferrihydrite, a nanocrystalline material. *Science* **2007**, *316* (5832), 1726−1729.
(21) U.S. Environmental Protection Agency. *EPA response to release of coal ash into the Dan River*. http://www.epa.gov/region4/duke-energy/ (accessed 2014).
(22) Howard, C. J.; Sabine, T. M.; Dickson, F. Structural and thermal parameters for rutile and anatase. *Acta Crystallogr.* **1991**, *B47*, 462−468.
(23) Kim, B.; Murayama, M.; Colman, B. P.; Hochella, M. F., Jr. Characterization and environmental implications of nano- and larger TiO(2) particles in sewage sludge, and soils amended with sewage sludge. *J. Environ. Monit.* **2012**, *14* (4), 1129−37.
(24) Luo, Z.; Wang, Z.; Li, Q.; Pan, Q.; Yan, C.; Liu, F. Spatial distribution, electron microscopy analysis of titanium and its correlation to heavy metals: Occurrence and sources of titanium nanomaterials in surface sediments from Xiamen Bay, China. *J. Environ. Monit.* **2011**, *13* (4), 1046−1052.
(25) Fang, J.; Shan, X. Q.; Wen, B.; Lin, J. M.; Owens, G.; Zhou, S. R. Transport of copper as affected by titania nanoparticles in soil columns. *Environ. Pollut.* **2011**, *159* (5), 1248−1256.
(26) Yang, H.; Lu, R.; Downs, R. T.; Costin, G. Goethite, alpha-FeO(OH), from single-crystal data. *Acta Crystallogr.* **2006**, *E62*, i250−i252.
(27) Blake, R. L.; Hessevick, R. E.; Zoltai, T.; Finger, L. W. Refinement of the hematite structure. *Am. Mineral.* **1966**, *51*, 123−129.
(28) Oliveira, M. L.; Marostega, F.; Taffarel, S. R.; Saikia, B. K.; Waanders, F. B.; DaBoit, K.; Baruah, B. P.; Silva, L. F. Nano-mineralogical investigation of coal and fly ashes from coal-based captive power plant (India): An introduction of occupational health hazards. *Sci. Total Environ.* **2014**, *468−469*, 1128−1137.
(29) U.S. Environmental Protection Agency. *Eden North Carolina coal ash spill ash results*; 2014. http://epa.gov/region4/duke-energy/ash/FINALwMaps-2014-0206-Ash-Sample-Team-1.pdf (accessed 2014).
(30) U.S. Environmental Protection Agency. *Eden North Carolina coal ash spill sediment results*; 2014. http://epa.gov/region4/duke-energy/sediment/Final-w-Maps-2014-0208-Sediment-Team2.pdf (accessed 2014).
(31) *Protocol for Derivation of Canadian Sediment Guidelines for Protection of Aquatic Life*; CCME-EPC-98E; Prepared by Environment Canada Guidelines Division, Technical Secretariat of CCME Task Group on water quality guidelines: Otawa, Canada. CCME. 1999. http://ceqg-rcqe.ccme.ca/download/en/226/ (accessed 2014).
(32) Pandey, V. C.; Singh, J. S.; Singh, R. P.; Singh, N.; Yunus, M. Arsenic hazards in coal fly ash and its fate in Indian scenario. *Resour. Conserv. Recycl.* **2011**, *55* (9−10), 819−835.
(33) Belkin, H. E.; Zheng, B.; Finkelmann, R. B. Human health effects of domestic combustion of coal in rural China: a causal factor for arsenic and fluorine poisoning. In *2nd World Chinese Conference on Geological Sciences Extended Abstracts*; Stanford University: Stanford, CA, 2000; pp 522−524.
(34) Huggins, F. E.; Senior, C. L.; Chu, P.; Ladwig, K.; Huffman, G. P. Selenium and arsenic speciation in fly ash from full-scale coal-burning utility plants. *Environ. Sci. Technol.* **2007**, *41*, 3284−3289.
(35) Jegadeesan, G.; Al-Abed, S. R.; Pinto, P. Influence of trace metal distribution on its leachability from coal fly ash. *Fuel* **2008**, *87* (10−11), 1887−1893.
(36) Guo, X.; Zheng, C. G.; Xu, M. H. Characterization of arsenic emissions from a coal-fired power plant. *Energy Fuels* **2004**, *18*, 1822−1826.
(37) Goldberg, S.; Johnston, C. T. Mechanisms of arsenic adsorption on amorphous oxides evaluated using macroscopic measurements, vibrational spectroscopy, and surface complexation modelling. *J. Colloid Interface Sci.* **2001**, *234*, 204−216.
(38) Swartz, C. H.; Blute, N. K.; Bardruzzman, B.; Ali, A.; Brabander, D.; Jay, J.; Besancon, J.; Islam, S.; Hemond, H. F.; Harvey, H. C. Mobility of arsenic in a Bangladesh aquifer: Inferences from geochemical profiles, leaching data, and mineralogical characterization. *Geochimica. Cosmochim. Acta* **2004**, *68*, 4539−4557.
(39) Erbs, J. J.; Berquó, T. S.; Reinsch, B. C.; Lowry, G. V.; Banerjee, S. K.; Penn, R. L. Reductive dissolution of arsenic-bearing ferrihydrite. *Geochimica. Cosmochim. Acta* **2010**, *74* (12), 3382−3395.
(40) Bose, P.; Sharma, A. Role of iron on controlling speciation and mobilization of arsenic in subsurface environment. *Water Res.* **2002**, *36*, 4916−4926.
(41) Duker, A. A.; Carranza, E. J. M.; Hale, M. Arsenic geochemistry and health. *Environ. Int.* **2005**, *31*, 631−641.
(42) Bauer, M.; Blodau, C. Mobilization of arsenic by dissolved organic matter from iron oxides, soils and sediments. *Sci. Total Environ.* **2006**, *354* (2−3), 179−190.
(43) Bauer, M.; Blodau, C. Arsenic distribution in the dissolved, colloidal and particulate size fraction of experimental solutions rich in dissolved organic matter and ferric iron. *Geochimica. Cosmochim. Acta* **2009**, *73* (3), 529−542.
(44) Grafe, M.; Erick, M. J.; Grossl, P. R.; Saunders, A. M. Adsorption of arsenate and arsenite on ferrihydrite in the presence and absence of dissolved organic carbon. *J. Environ. Qual.* **2002**, *31*, 1115−1123.
(45) Cudennec, Y.; Lecerf, A. The transformation of ferrihydrite into goethite or hematite, revisited. *J. Solid State Chem.* **2006**, *179* (3), 716−722.
(46) Michel, F. M.; Barron, V.; Torrent, J.; Morales, M. P.; Serna, C. J.; Boily, J. F.; Liu, Q.; Ambrosini, A.; Cismasu, A. C.; Brown, G. E., Jr. Ordered ferrimagnetic form of ferrihydrite reveals links among structure, composition, and magnetism. *Proc. Natl. Acad. Sci. U.S.A.* **2010**, *107* (7), 2787−2792.
(47) Schwertmann, U.; Stanjek, H.; Becher, H. H. Long-term in vitro transformation of 2-line ferrihydrite to goethite/hematite at 4, 10, 15 and 25°C. *Clay Miner.* **2004**, *39* (4), 433−438.

DOI: 10.1021/es505662q
Environ. Sci. Technol. 2015, 49, 3375−3382

(48) Gondikas, A. P.; von der Kammer, F.; Reed, R. B.; Wagner, S.; Ranville, J. F.; Hofmann, T. Release of TiO_2 nanoparticles from sunscreens into surface waters: A one-year survey at the old Danube recreational lake. *Environ. Sci. Technol.* **2014**, *48* (10), 5415−5422.
(49) Sayes, C. M.; Wahi, R.; Kurian, P. A.; Liu, Y.; West, J. L.; Ausman, K. D.; Warheit, D. B.; Colvin, V. L. Correlating nanoscale titania structure with toxicity: A cytotoxicity and inflammatory response study with human dermal fibroblasts and human lung epithelial cells. *Toxicol. Sci.* **2006**, *92*, 174−185.
(50) Petkovic, J.; Zegura, B.; Stevanovic, M.; Drnovsek, N.; Uskokovic, D.; Novak, S.; Filipic, M. DNA damage and alterations in expression of DNA damage responsive genes induced by TiO_2 nanoparticles in human hepatoma HepG2 cells. *Nanotoxicology* **2011**, *5*, 341−353.
(51) Shukla, R. K.; Kumar, A.; Gurbani, D.; Pandey, A. K.; Singh, S.; Dhawan, A. TiO(2) nanoparticles induce oxidative DNA damage and apoptosis in human liver cells. *Nanotoxicology* **2013**, *7* (1), 48−60.
(52) Binh, C. T.; Tong, T.; Gaillard, J. F.; Gray, K. A.; Kelly, J. J. Common freshwater bacteria vary in their responses to short-term exposure to nano-TiO_2. *Environ. Toxicol. Chem.* **2014**, *33* (2), 317−327.
(53) Tong, T.; Binh, C. T.; Kelly, J. J.; Gaillard, J. F.; Gray, K. A. Cytotoxicity of commercial nano-TiO_2 to *Escherichia coli* assessed by high-throughput screening: Effects of environmental factors. *Water Res.* **2013**, *47* (7), 2352−2362.
(54) Fan, W.; Cui, M.; Liu, H.; Wang, C.; Shi, Z.; Tan, C.; Yang, X. Nano-TiO_2 enhances the toxicity of copper in natural water to *Daphnia magna*. *Environ. Pollut.* **2011**, *159* (3), 729−734.

■ NOTE ADDED AFTER ASAP PUBLICATION

There was an error in Figure 3 in the version of this paper published February 25, 2015; the corrected version published March 17, 2015.

DOI: 10.1021/es505662q
Environ. Sci. Technol. 2015, 49, 3375−3382